e-ISSN: 2250-0758 | p-ISSN: 2394-6962
Volume-12, Issue-6, (December 2022)
https://doi.org/10.31033/ijemr.12.6.13

Numerical Simulation of Two-Dimensional Shear Flow

K. Sreeram Reddy
Department of Mathematics, Osmania University, Hyderabad, Telangana-500007, INDIA

Corresponding Author: dr_sreeram_reddy@yahoo.com

ABSTRACT

Numerical experiments on finite difference solutions of time dependent two-dimensional Navier-Stokes equations are used to study the transition triggering off in a mixing layer of initial tanh(y) profile. The inflow is excited by sinusoidal waves resulting from the linear theory of hydrodynamic instability. Numerical realizations are compared, through stream wise growth of momentum thickness and vorticity plots, with Winant and Browand experiments.

The transition control and triggering off are studied through the finite difference solution of the two-dimensional time dependant Navier-Stokes equations. In a shear flow, the transition results from hydrodynamic amplification of unstable disturbances stimulated by perturbations of diverse origin. In a unidirectional flow, the most unstable disturbances are two-dimensional transverse waves {2, 3} and experiments have shown the area where small disturbances grow exponentially {5,8,9,10}. Thus, a two dimensional numerical simulation is well suited to the study of transition triggering off.

Keywords-- Mean Velocity, Reynolds Number, Simulation, Momentum Thickness, Eigen Functions

Nomenclature:

U	General Translation Velocity	α_r	Wave Number
d	Characteristic length	β	Angular Frequency
$\bar{u}$	Mean Velocity	c	Phase Velocity
R_x, R_θ	Reynolds Numbers	ω	vorticity
λ	Wave length	ψ	stream function

I. NUMERICAL SIMULATION DESCRIPTION

The simulation field is rectangular Fig. 1. We consider a mixing layer, with an initial mean velocity profile:

$$\bar{u} = U + \frac{\delta U}{2}\tanh\left(\frac{y}{d}\right) \qquad (1)$$

Where δU is the velocity difference between the two layers and chosen as velocity scale, U the general translation velocity, and d a characteristic length. In the dimensionless problem, with δU =d =1, the momentum thickness is θ_0 =0.5. At upstream boundary, x=0 a second condition $\frac{\delta v}{\delta x} = 0$ is imposed on mean velocity. On this limit, some unsteady disturbances could be possibly superimposed. For the two lateral boundaries, y = +h/2 reflection conditions $\frac{\delta u}{\delta x} = 0$, $\bar{v} = 0$ are used in order to simulate free shear boundaries. At x = 1, the outflow conditions are simply v = 0, $\frac{\delta v}{\delta x} = 0$ for instantaneous velocity.

The Navier-Stokes equations are formulated in terms of the stream function ψ and vorticity $\omega = -\nabla^2\psi$ and discretized over a grid of square meshes $\delta x = \delta Y$. The vorticity advection is approached by an implicit second order scheme 7 which conserves both voritcity and square vorticity. In association with classical five points scheme for the Laplacian operator of Poisson's equation for ψ, this scheme also conserves kinetic energy $(\nabla\psi)^2/2$. In order to keep these important conservation properties for ω in present numerical simulations, the viscous diffusion is approached by a scheme of Crank-Nikolson type. The numerical code being designed in this way, the parabolic growth of a laminar mixing layer for the zero perturbation case is accurately described. After this check the code is used for the simulation of transition. A mixing layer of constant thickness is always unstable for sufficiently large transversal waves, whatever be the value of the Reynolds number $R_\theta = \delta U\theta_0/v = 1/2v$, {1}. This result transposed in the present spatial growing case, suggests that any unsteady disturbances on the upstream boundary having energy in the low frequency range shall trig-ger off the transition into the simulation field. In order to reduce the computation field size and simultaneously the simulation cost, the inflow is excited with the most unstable wave for an hyperbolic tangent mean velocity profile. which is represented in dimensionless form :

e-ISSN: 2250-0758 | p-ISSN: 2394-6962
Volume-12, Issue-6, (December 2022)
https://doi.org/10.31033/ijemr.12.6.13

$$\psi(O,y,t) = \psi(O,y) + \epsilon(\psi_R(y)\cos\beta t + \psi_I(y)\sin\beta t)$$

ψ_I, ψ_R (Fig. 1), are imaginary and real parts of normalized eigen function, β is the angular frequency of this wave depending on the similitude parameters U and R_θ . Eigen functions for growing spatial case has been numericaly calculated by Michalke 4 for the case $U = 0.5$, $R_\theta = \infty$. In this case the features of the unstable disturbance are, a wave-number $\alpha_r = 0.43129$ a phase velocity C = 0.5127, an angular frequency $\beta = \alpha_r C$ and a growth rate $-\alpha_i = 0.228425$. These ψ_R, ψ_I, α_r values can be used in finite difference computations for other values of U and R_θ on condition that new angular frequency β are fixed with a U corrected Phase velocity C, on the assumption that eigen-modes, for a moving observator at U velocity, are practically independent of the parameters U and R_θ.

II. RESULTS

Numerical experiments has been done for a general translation velocity U = 1.0496 accord- ing to the experimental parameters of Winant and Browand 8. For this case, the corrected frequency is $\beta = 0.4282$. A grid of 118x32 square meshes, $\delta X = 1$, has been used. The thickness $\delta_{0.99}$ of the hyperbolic tangent profile is discretized by five points and the perturbation wave length $\lambda = 2\pi/\alpha_r$ by approximately 15 points. The computed field is about8 wavelength λ long. There is about 23 time steps fixed at $\delta t = \delta X/(0.5 + U) = 0.667$, for one perturbation period.

The first realisation R_5 is calculated for $R_\theta = 12.5$, the amplitude of imposed perturba- tion $\epsilon = 0.03$ is inferred from experimental values of root-mean square velocity {8}. The realization reaches a steady state at a dimensionless time of about t = 200. The config- uration of the resulting flow is basically laminar. The growth of momentum thickness is parabolic according to experiments and theory, Fig. 2.

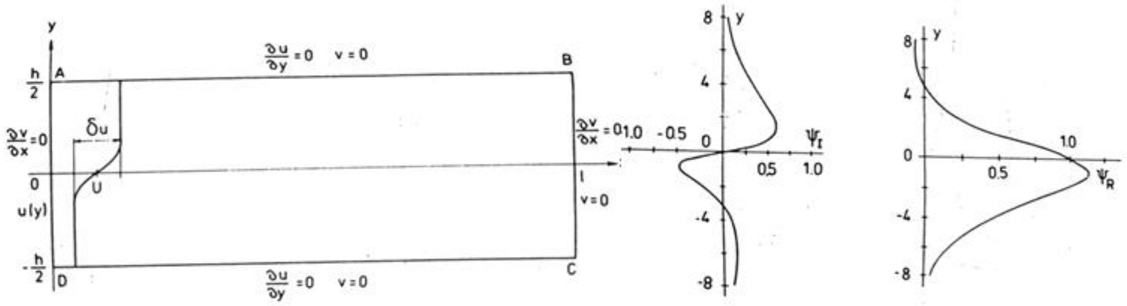

Figure 1: Left: Simulation domain grometry and steady boundary conditionsRight: Eigen-functions of most unstable disturbance from Michalke

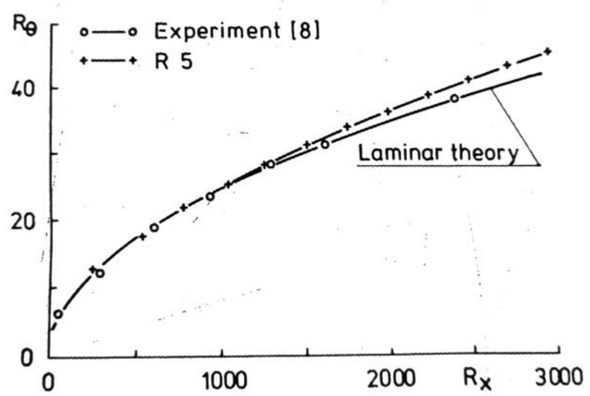

Figure 2: Stream wise growth of momentum thickness θ(x), R_θ, R_x; laminar Reynolds range

One other realization R_6 has been done for $R_\theta = 40$ and $\epsilon = 0.141$. This Reynolds value is related to the onset of the transition in experiments above which the momentum thickness $\theta(x)$ growth becomes linear. Contrary to experiments the strem wise amplification disturbance is quickly bounded by the non-linear

e-ISSN: 2250-0758 | p-ISSN: 2394-6962
Volume-12, Issue-6, (December 2022)
https://doi.org/10.31033/ijemr.12.6.13

interactions. A steady of vortex cores passed through the computed field without vortex merging Fig. 4a. The growth of $\theta(x)$ remains parabolic in an over-saturated laminar configuration Fig. 3, this result seems to confirm the existence of finite amplitude steady state {3, 6}.

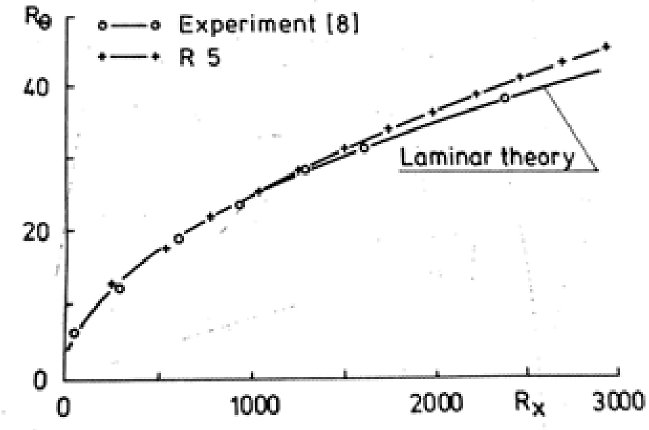

Figure 3: Stream wise growth of momentum thickness $\theta(x)$, transitional Reynolds range

The whole picture changes when there is a noisy disturbance in the flow. The R_8 realization duplicates R_6 with a Gaussian noise of .05 standard deviation superimposed on inflow excitation function. Then the structure of the computed flow Fig. 4b is totally different. We observe an unstable vorticity sheet which gives rise to a row of rolling-up vortices. This configuration change, is also observed on the stream wise growth of momentum thickness θ, Fig. 3, which deviates from the laminar regions to catch up with the domainof linear experimental variation.

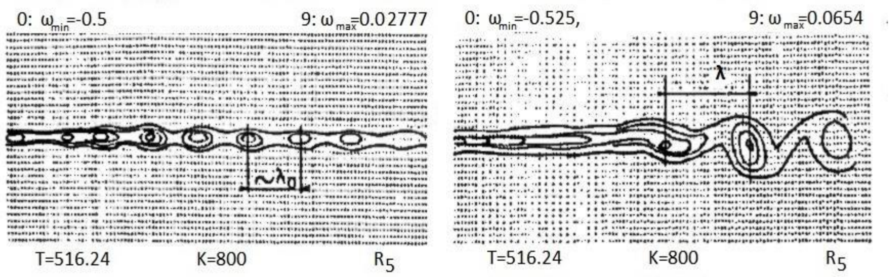

Figure 4: Printer iso-vorticity plot:(a): without noise R_6(b): with Gaussian noise on excitation R_8

REFERENCES

[1] R. Betchov & A. Szewczyk. (1963). Stability of a shear layer between parallel streams. *Phys. of Fluid, 6*(1), 1391-1396.
[2] A. Michalke. (1964). On the inviscid unstability of the hyperbolic tangent velocity profile. *J. of Fluid Mech., 19,* 543-556.
[3] H. Shade (1964). Contribution to the non linear stability theory of inviscid shear layers. *Phys. of Fluid, 7*(5), 623-628.
[4] A. Michalke. (196). On spatially growing disturbance in an inviscid shear layer. *J. of Fluid Mech., 23*(3), 521-544.
[5] P. Freymuth, (1966). On transition in seperated laminar boundary layer. J. of Fluid Mech., 25(4), 683-670.
[6] J.J. Stuart. (1967). On finite amplitude oscillations in laminar mixing layers. *J. of Fluid Mech., 29*(1), 417-440.
[7] A. Arakawa. (1970). Numerical solution of large scale atmospheric motions. *SIAM AMS Proc., 2,* pp. 24-40.
[8] C.D Winant & F.K. Brownd. (1974). Vortex pairing : the mechanism of turbulent mixing layer, growth at moderate Reynolds number. *J. of Fluid Mech., 63*(2), 237-255.
[9] A.Roshko. (1976. Structure of turbulence shear flow, a new look. AIAA J., 14(10), 1349.
[10] I. Wygnanski, D.Oster, H. Fielder & B. Dziomba. (1979). On the perseverence of quasi di-mensional eddy structure at a turbulent mixing layer. *J. of Fluid Mech., 93*(2), 325-335.
[11] Mahesh, Ch. (2020). The 3-point quadrature rules with constant weight function. *Asian-European Journal of Mathematics, 13*(02). Available at: https://doi.org/10.1142/S1793557120500412.